

Ferrocenedicarboxylic Acid Modified Multiwall Carbon Nanotubes Paste Electrode for Voltammetric Determination of Sulfite

Ali A. Ensafi* and Hassan Karimi-Maleh

Department of Chemistry, Isfahan University of Technology, Isfahan 84156–83111, Iran

*E-mail: Ensafi@cc.iut.ac.ir

Received: 6 March 2010 / Accepted: 15 March 2010 / Published: 31 March 2010

The electrocatalytic oxidation of sulfite has been studied by ferrocenedicarboxylic acid modified carbon nanotubes paste electrode. It has been found that under the optimum condition (pH 7.0) in cyclic voltammetry, the oxidation of sulfite is occurred at a potential about 350 mV less positive than that an unmodified carbon nanotubes paste electrode. The kinetic parameters such as electron transfer coefficient, α , and the catalytic reaction rate constant, k'_h , were also determined using electrochemical approaches. Also, electrochemical impedance spectroscopy used for study behavior of sulfite in aqueous solution. Using differential pulse voltammetric (DPV) method, the electrocatalytic oxidation peak current of sulfite shows a linear calibration curve in the range $0.6 - 100 \mu\text{mol L}^{-1}$ of sulfite concentration. The detection limit (3σ) was determined as $0.3 \mu\text{mol L}^{-1}$ by DPV method. The $RSD\%$ for 10.0 and $30.0 \mu\text{mol L}^{-1}$ sulfite was 2.1% and 1.8%, respectively. The proposed method was examined as a selective, simple and precise method for voltammetric determination of sulfite in real samples with satisfactory results.

Keywords: Sulfite determination, Electrochemical impedance spectroscopy, Carbon nanotubes paste electrode, Electrocatalytic, Ferrocenedicarboxylic acid, Voltammetry.

1. INTRODUCTION

As is known, sulfite is a typical example of sulfur oxoanions. The determination of sulfite (or sulfur dioxide) is important in many environmental and industrial situations, particularly when monitoring atmosphere [1,2], foods and beverages[3,4], process liquors and wastewaters from paper mills[5], photographic laboratories[6,7] and mining sites[8]. Several methods have been proposed for the determination of sulfite including titration [9], high-performance liquid chromatography [10], capillary electrophoresis [11–13], spectrophotometry [14,15], chemiluminescence method [16,17],

flow injection analysis [18,19] and electrochemical methods [20–26]. Many of them are not enough sufficiently sensitive and/or are time consuming and/or used expensive instrumentations. The comparison of the proposed method for sulfite determination with other published papers is given in Table I.

Table I. Comparison of the efficiency of some methods in the determination of sulfite.

Method	<i>pH</i>	Limit of detection ($\mu\text{mol L}^{-1}$)	Linear dynamic range ($\mu\text{mol L}^{-1}$)	Reference
CE ^a	8.2	2	10–800	12
Amperometry	8.0	2.8	5–1500	20
Cyclic Voltammetry	5.5	80	250–2380	21
DPV ^b	8.0	0.21	4–443	22
LSV ^c	7.0	3	5–60	23
Amperometry	6.2	3	4–200	24
DPV	8.0	0.1	4–100	25
Chronoamperometry	6.0	1.2	4–69	26
Cyclic Voltammetry	7.0	40	1300–7200	27
Amperometry	11.0	Not reported	10000–30000	28
Cyclic Voltammetry	11.0	Not reported	20000–100000	29
DPV ^b	7.0	0.3	6–100	This work

^a Capillary electrophoresis.

^b Differential pulse voltammetry.

^c Linear Sweep Voltammetry

Carbon nanotubes can be used to promote electron transfer reactions when used as electrode material in electrochemical devices, electrocatalysis and electroanalysis processes due to their significant mechanical strength, high electrical conductivity, high surface area, good chemical stability, as well as relative chemical inertness in most electrolyte solutions and a wide operation potential window [30]. The electronics properties of these nano-materials have been exploited as means of promoting the electron transfer reaction for a wide range of molecules and biological species including; insulin[31], carbohydrates [32], hydrogen peroxide [33], glucose [34], norepinephrine [35], aminophenol [36], morin [37], cytochrome C [38], promethazine [39], thiols [40], methyldopa [41], epinephrine [42] and nicotinamide adenine dinucleotide [43].

In this study in continuation of our studies concerning the preparation of chemically modified electrodes [44–47], we described initially the preparation and suitability of a ferrocenedicarboxylic acid modified carbon nanotubes paste electrode (FDCAMCNTPE) as a new electrocatalyst in the electrocatalysis and determination of sulfite in an aqueous buffer solution. Finally, in order to demonstrate the catalytic ability of the modified electrode in the determination of sulfite in real samples, we examined this method for the voltammetric determination of sulfite in weak liquor from the wood and paper industry.

2. EXPERIMENTAL PART

2.1. Chemicals

All chemicals used were of analytical reagent grade. Doubly distilled water was used throughout. Ferrocenedicarboxylic acid was used from Fluka and sodium sulfite from Merck, all used as received.

Universal buffer (boric acid, phosphoric acid, acetic acid plus sodium hydroxide, 0.04 mol L⁻¹) solutions with different *pH* values were used.

High viscosity paraffin ($d = 0.88 \text{ Kg L}^{-1}$) from Merck was used as the pasting liquid for the preparation of carbon paste electrode. Graphite powder (particle diameter = 0.10 mm) and carbon nanotubes (>90% MWCNT basis, $d \times l = (110\text{--}70 \text{ nm}) \times (5\text{--}9 \text{ }\mu\text{m})$) from Fluka were used as the substrate for the preparation of the carbon paste electrode as a working electrode.

Spectrally pure graphite powder (particle size < 50 μm) and high viscose paraffin oil (density = 0.88 Kg L⁻¹) from Merck were used for the preparation of the carbon paste electrode (CPE).

2.2. Apparatus

Cyclic voltammetry (CV), chronoamperometry, and differential pulse voltammetry (DPV) were performed in an analytical system, Autolab with PGSTAT 12 (Eco Chemie B. V., Utrecht, and The Netherlands). The system was run on a PC using GPES and FRA 4.9 software. For impedance measurements, a frequency range of 100 kHz to 0.10 Hz was employed. The AC voltage amplitude used was 5 mV, and the equilibrium time was 10 minutes. A conventional three-electrode cell assembly consisting of a platinum wire as an auxiliary electrode and an Ag/AgCl (KCl_{sat}) electrode as a reference electrode was used. The working electrode was either an unmodified carbon nanotubes paste electrode (CNPE) or a carbon nanotubes paste electrode modified with ferrocenedicarboxylic acid (FDCAMCNTPE). The prepared electrodes with carbon nanotubes and with the modifier were characterized by scanning electron microscopy (SEM).

A *pH*-meter (Corning, Model 140) with a double junction glass electrode was used to check the *pH* of the solutions.

2.3. Preparation of the electrode

Ferrocenedicarboxylic acid (0.010 g) was dissolved in 10 mL diethyl ether and hand mixed with 0.89 g graphite powder plus 0.10 g carbon nanotubes in a mortar and pestle. The solvent was evaporated by stirring. Using a syringe, 0.88 g paraffin was added to the mixture and mixed well for 40 min until a uniformly-wetted paste was obtained. The paste was then packed into a glass tube. Electrical contact was made by pushing a copper wire down the glass tube into the back of the mixture. When necessary, a new surface was obtained by pushing an excess of the paste out of the tube and polishing it on a weighing paper. The unmodified carbon paste electrode (CPE) was prepared in the

same way without adding ferrocenedicarboxylic acid and carbon nanotubes to the mixture to be used for comparison purposes.

2.4. Preparation of weak liquor

The weak liquor from a wood and paper factory of Mazandaran province in Iran prepared and diluted 10–time with water. Then, 1.0 mL of the solution plus 9 mL of the buffer (*pH* 7.0) were used for the analysis of sulfite contents with standard addition method.

2.5. Preparation of boiler water

Without any pre-treatment of the sample, an accurate volume of the boiler water depending on the amount of sulfite in the sample (commonly 0.2–1.0 mL) directly was subjected for voltammetric measurement of sulfite as recommended procedure.

3. RESULTS AND DISCUSSION

3.1. SEM characterization of multiwall carbon nanotubes (MWCNTs)

Figure (1) displays a typical morphology of the modified multiwall carbon nanotubes paste electrode with ferrocenedicarboxylic acid (a) and the unmodified carbon paste electrode (b) characterized by SEM. As shown in Figure 1, ferrocenedicarboxylic acid on the surface of CNTs did not change the morphology of CNTs, but made it more compact. However, it can be clearly seen that MWCNTs dispersed homogeneously.

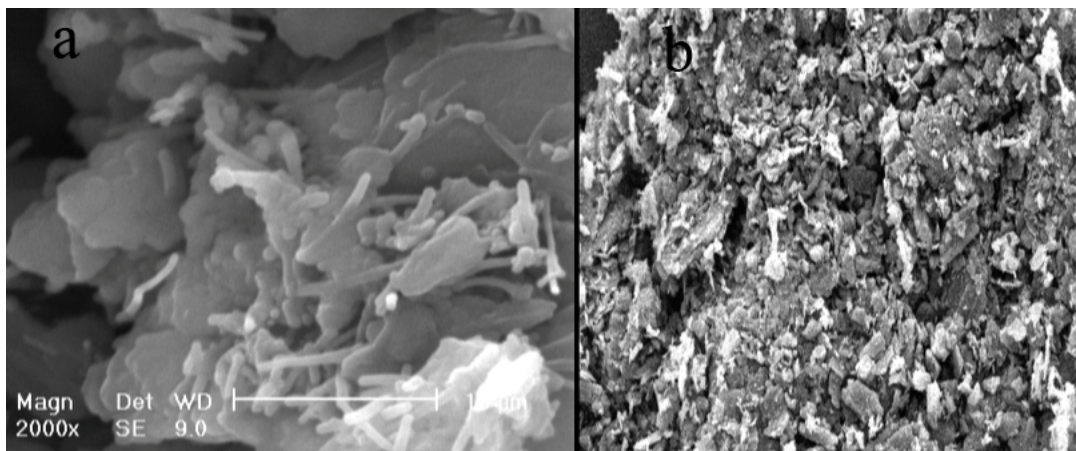


Figure 1. SEM image of a) FDCAMCNTPE, and b) the unmodified electrode.

3.2. Electrochemistry of mediator

The electrochemical properties of the modified electrode were studied by cyclic voltammetry in a buffer solution ($pH\ 7.0$). The experimental results showed a well-defined and reproducible anodic and cathodic peaks related to Fc/Fc^+ redox couple with quasi-reversible behavior, with peak separation potential of ΔE_p ($E_{pa}-E_{pc} = 100\ mV$). These cyclic voltammograms were used to examine the variation of the peak currents vs. the potential scan rates. The plots of the anodic and cathodic peak currents were linearly dependent on $v^{1/2}$ at the all scan rates. This behavior indicates that the nature of redox process is diffusion controlled [47].

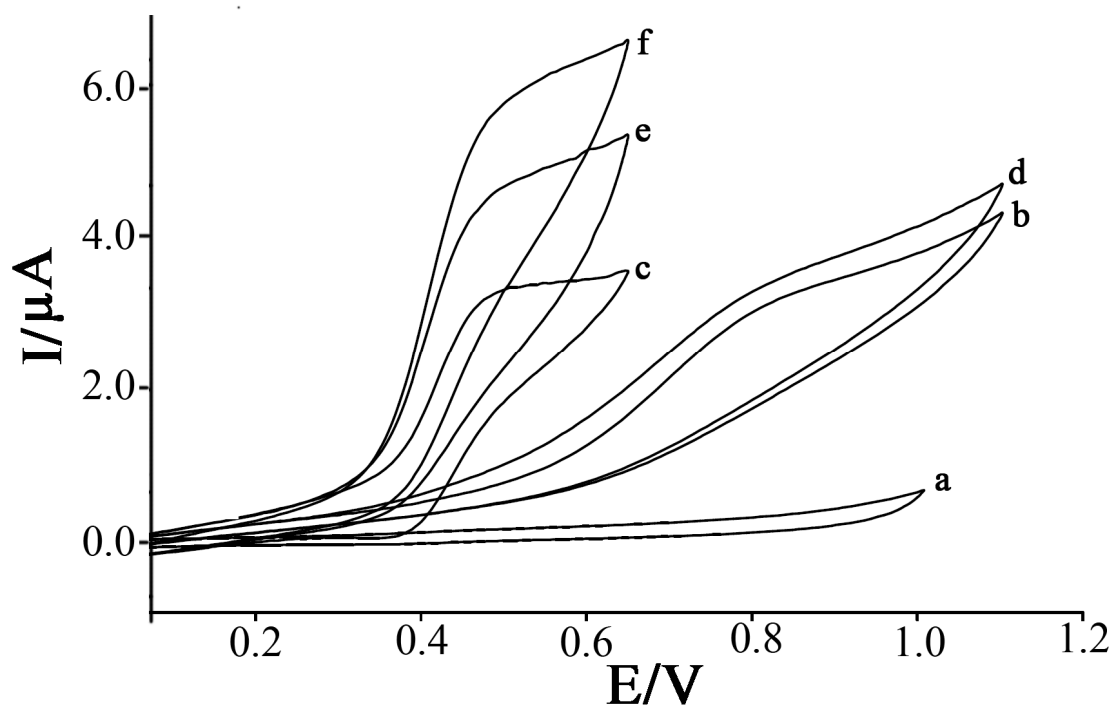


Figure 2. Cyclic voltammograms of (a) CPE in $0.04\ mol\ L^{-1}$ universal buffer ($pH\ 7.0$) at scan rate $10\ mV\ s^{-1}$ and (b) as (a) plus $1000\ \mu mol\ L^{-1}$ sulfite; (c) as (a) and (d) as (b) at the surface of FDCAMCNTPE and CNPE respectively. Also (e) and (f) as (b) at the surface of FDCAMCPE and FDCAMCNTPE, respectively.

3.3. Electrochemistry of sulfite at FDCAMCNTPE

Figure 2 depicts the cyclic voltammetric responses from the electrochemical oxidation of $1000\ \mu mol\ L^{-1}$ sulfite at FDCAMCNTPE (curve f), ferrocenedicarboxylic acid modified carbon paste electrode (FDAMCPE) (curve e), CNPE (curve d) and a bare CPE (curve b). However, peaks potential of (c) and (a) show FDCAMCNTPE behavior and a bare CPE behavior in the buffer solution. As can be seen, the anodic peaks potential for the oxidation of sulfite at FDCAMCNTPE (curve f) and at FDAMCPE (curve e) is about $480\ mV$, while at the CNPE (curve d) the peak potential is about $830\ mV$, whereas the peak potential at the bare CPE (curve b) is about $860\ mV$ for sulfite. From these

results, it is concluded that the best electrocatalytic effect for sulfite oxidation is observed at FDCAMCNTPE (curve f). For example, the results are shown that the peak potential of sulfite oxidation at FDCAMCNTPE (curve f) shifted by about 350 and 380 mV toward the less positive potential values compared with CNPE (curve d) and with a bare CPE (curve b), respectively. Similarly, when we compared the oxidation of sulfite at the FDAMCPE (curve e) and FDCAMCNTPE (curve f), there is a dramatic enhancement of the anodic peak current at FDCAMCNTPE relative to the value obtained at the FDAMCPE. This behavior is relative to combination of carbon nanotubes and mediator definitely improves the characteristics of sulfite oxidation.

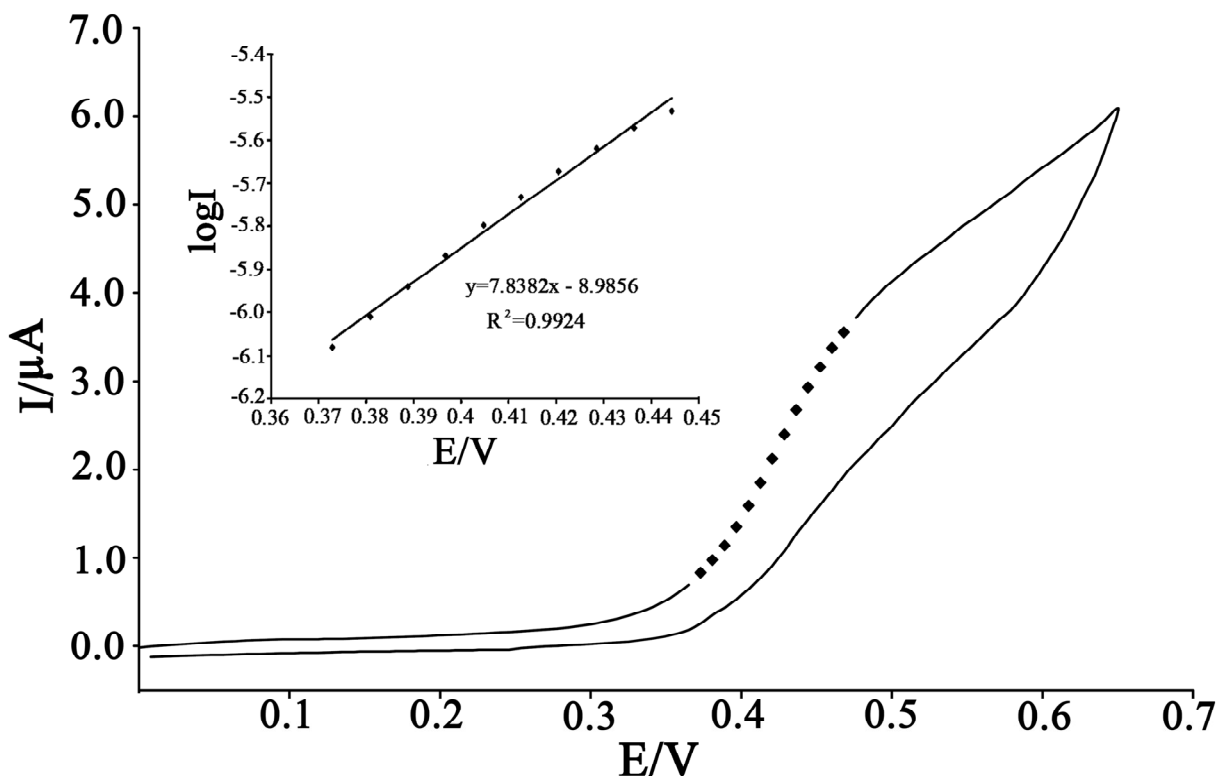


Figure 3. Tafel plot for FDCAMCNTPE in 0.04 mol L^{-1} universal buffer solution ($pH 7.0$) at a scan rate of 10 mV s^{-1} in the presence of $1000 \mu\text{mol L}^{-1}$ sulfite.

In order to obtain information on the rate determining step, a Tafel plot was developed for FDCAMCNTPE using the data derived from the raising part of the current–voltage curve (Figure 3). The slope of the Tafel plot is equal to $n(1-\alpha)F/2.3RT$ which comes up to $7.8382 \text{ V decade}^{-1}$. We obtained $n\alpha$ equal to 0.59. Assuming $n = 1$, then $\alpha = 0.59$. In addition, the value of an_α (n_α is the number of electrons involved in the rate determining step) was calculated for the oxidation of sulfite at $pH 7.0$ for both the modified and unmodified carbon nanotubes paste electrodes using the following Equation [48,49]:

$$an_\alpha = 0.048/(E_P - E_{P/2}) \quad (1)$$

where, $E_{P/2}$ is the potential corresponding to $I_{P/2}$. The values for an_a were found to be 0.60 and 0.22 at the surface of both FDCAMCNTPE and the unmodified carbon nanotubes paste electrode, respectively. Those values show that the over-potential of sulfite oxidation is reduced at the surface of FDCAMCNTPE, and also that the rate of electron transfer process is greatly enhanced. This phenomenon is, thus, confirmed by the larger I_{pa} values recorded during cyclic voltammetry at FDCAMCNTPE. In addition, with increasing the potential scan rate, the catalytic oxidation peak potential gradually shifts towards more positive potentials, suggesting a kinetic limitation in the reaction between the redox site of the ferrocenedicarboxylic acid and sulfite. However, the oxidation currents change linearly with the square root of the scan rate, suggesting that at sufficient over-potentials, the reaction is mass transfer controlled. The results show that the overall electrochemical oxidation of sulfite at the modified electrode might be controlled by the cross-exchange process between sulfite and the redox site of the ferrocenedicarboxylic acid and by the diffusion of sulfite.

3.4. Chronoamperometry study

For determination of the diffusion coefficient of sulfite, double potential step chronoamperometry was used with FDCAMCNTPE. Figure 4A shows the current–time curves of FDCAMCNTPE by setting the electrode potential at 700 mV (first step) and 250 mV (second step) vs. Ag|AgCl|KCl_{sat} for different concentration of sulfite. As can be seen, there is not any net anodic current corresponding to the oxidation of the mediator in the presence of sulfite. On the other hand, the forward and backward potential step chronoamperometry for the mediator in the absence of sulfite shows symmetrical chronoamperogram with an equal charge consumed for the reduction and oxidation of the ferrocenedicarboxylic acid at the surface of unmodified CPE (Figure 4B, a'). On the other hand, in the presence of sulfite, the charge value associated with forward chronoamperometry is significantly greater than that observed for backward chronoamperometry (Figure 5B, b'– d'). The linearity of the electrocatalytic current vs. $v^{1/2}$ shows that the current is controlled by diffusion of sulfite from the bulk solution toward the surface of the electrode that caused near Cottrellian behavior. Therefore, the slope of linear region of Cottrell's plot can be used to estimate the diffusion coefficient of sulfite. A plot of I vs. $t^{-1/2}$ for a FDCAMCNTPE in the presence of sulfite gives a straight line (Fig. 5A), which slope can be used to estimate the diffusion coefficient of sulfite (D) in the ranges of 200 to 800 $\mu\text{mol L}^{-1}$. The mean value of the D for sulfite was found to be $1.86 \times 10^{-6} \text{ cm}^2 \text{ s}^{-1}$.

The rate constant for the chemical reaction between sulfite and redox sites in FDCAMCNTPE, k_h , can be evaluated by chronoamperometry according to the method of Galus [50]:

$$I_C/I_L = \pi^{1/2} \gamma^{1/2} = \pi^{1/2} (k C_b t)^{1/2} \quad (2)$$

where I_C is the catalytic current of sulfite at the FDCAMCNTPE, I_L is the limited current in the absence of sulfite and t is the time elapsed (s). The above equation can be used to calculate the rate constant of the catalytic process k_h . Based on the slope of the I_C/I_L versus $t^{1/2}$ plots (Fig. 5B), k_h can be obtained for a given sulfite concentration. From the values of the slopes an average value of k_h was

found to be as $3.32 \times 10^2 \text{ mol}^{-1} \text{ L s}^{-1}$. The value of k_h explains as well as the sharp feature of the catalytic peak observed for catalytic oxidation of sulfite at the surface of FDCAMCNTPE.

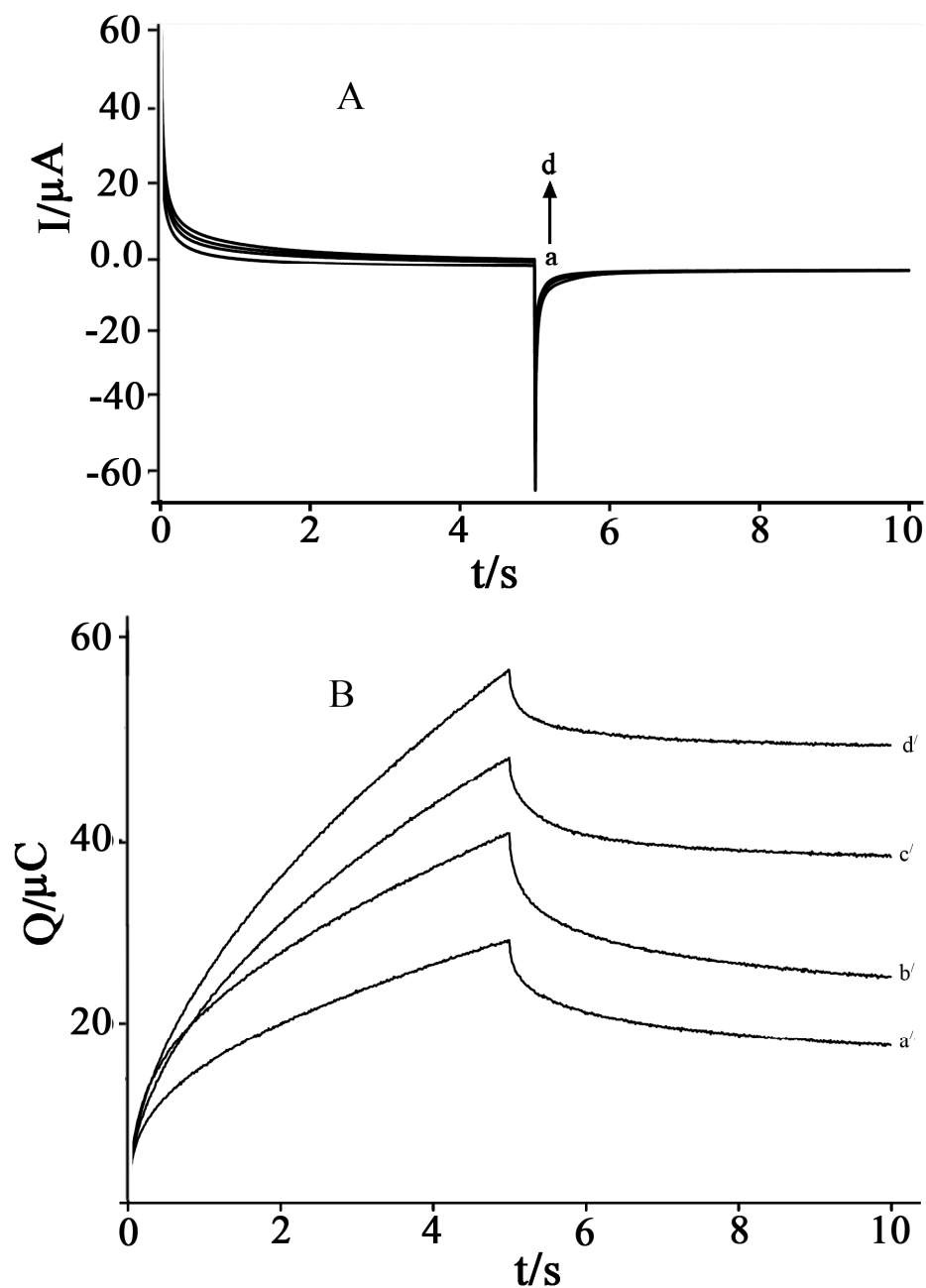


Figure 4. A): Chronoamperograms obtained at the FDCAMCNTPE in the absence a) and presence of b) 200, c) 500 and d) 800 $\mu\text{mol L}^{-1}$ of sulfite in the buffer solution (pH 7.0). First and second potential steps were corresponds of 0.70 and 0.25 V vs. Ag/AgCl. B): Charge-time curves: a' for curve a, b' for curve b, c' for curve c, and d' for curve d.

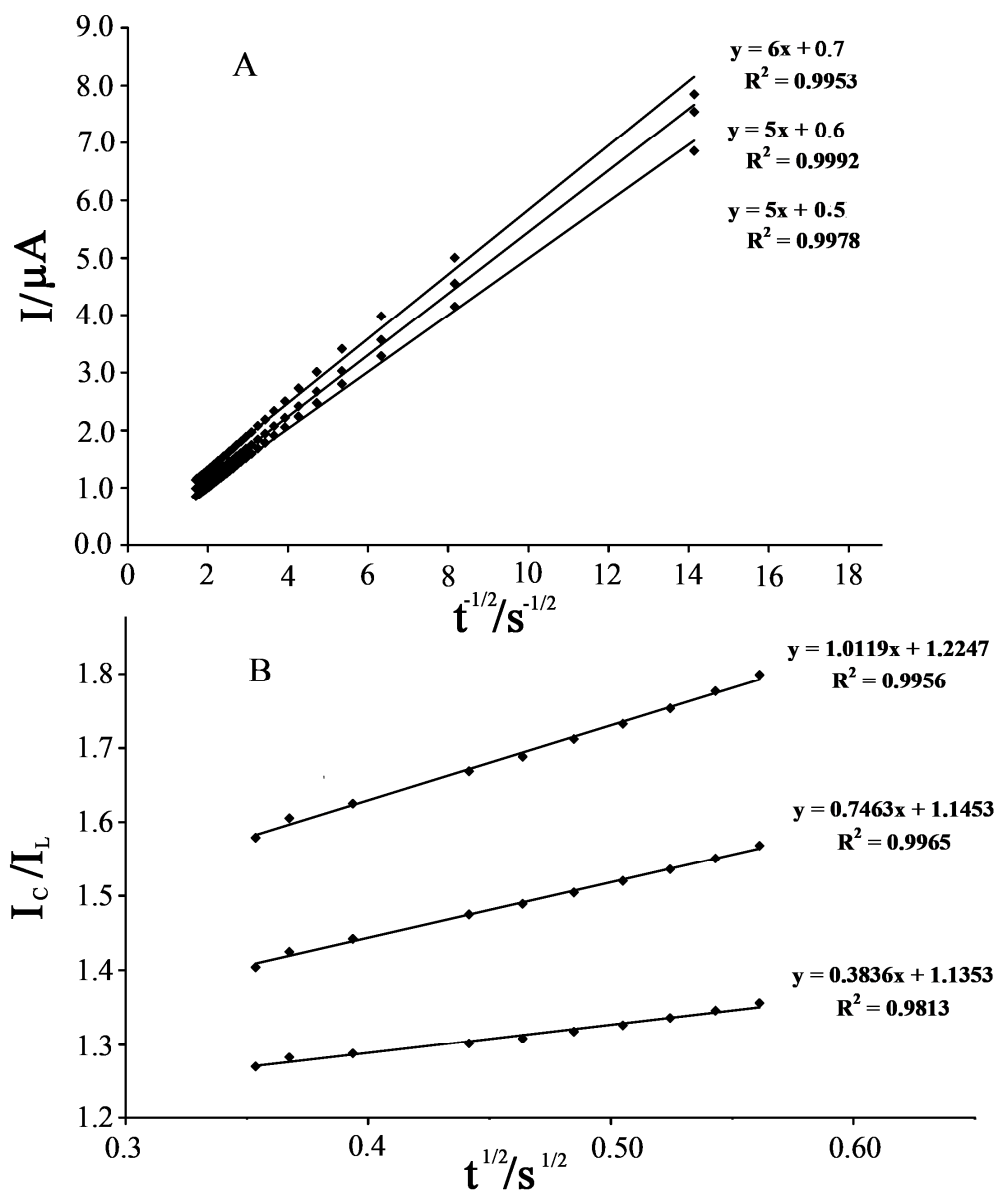
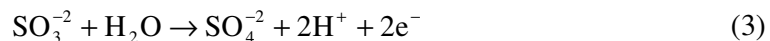


Figure 5. A) Cottrell's plot for the data from the chronoamperograms. B) Dependence of I_C/I_L on $t^{1/2}$ driven from the chronoamperograms data.

3.5. Influence of pH

In order to optimize the electrocatalytic response of the sensor to sulfite oxidation, we investigated the effect of pH on the electrocatalytic oxidation of sulfite in 0.04 mol L^{-1} universal buffer solutions with different pH values ($4.0 < pH < 9.0$) at the surface of FDCAMCNTPE using cyclic voltammetry. The influence of pH on the both peaks current and peaks potential were assessed through

examining the electrode response in the buffer solutions. It well known that the electrochemical behavior of sulfite is dependent on pH value of the aqueous solution, as shown in Eq. 3:



On the other hand, the electrochemical property of Fc/Fc^+ redox couple is independent of the solution pH [45,47]. The variation of I_{pa} vs. pH is shown in Figure 6. The results showed that the maximum electrocatalytic current was obtained at pH 7.0. Therefore, pH 7.0 was chosen as the optimum pH for the determination of sulfite at FDCAMCNTPE.

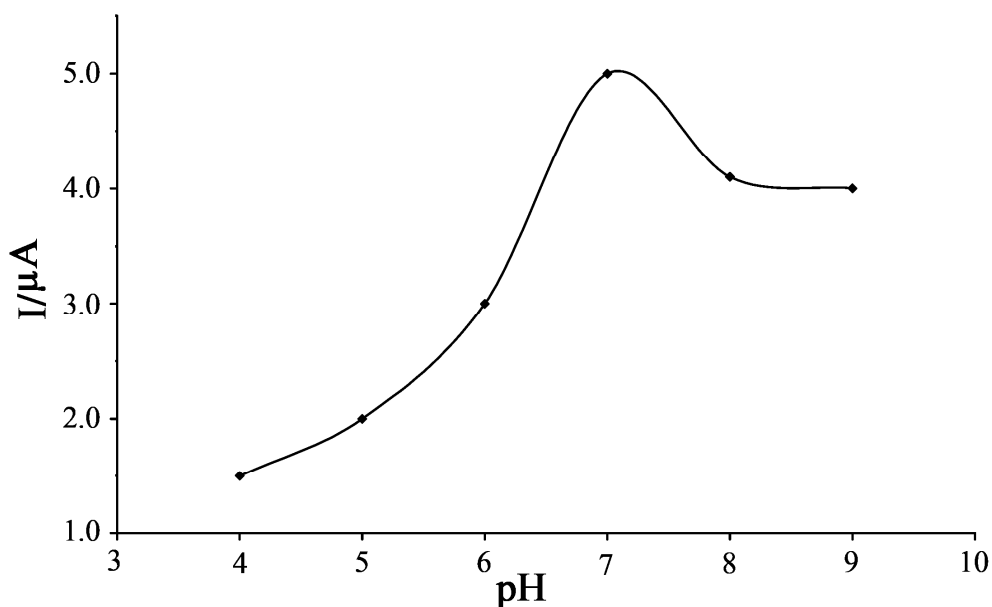


Figure 6. Current- pH curves for electro-oxidation of $900 \mu\text{mol L}^{-1}$ sulfite the buffer solution with various pH values at the surface of FDCAMCNTPE with a scan rate 10 mV s^{-1} .

3.6. Electrochemical impedance spectroscopy studies

Electrochemical impedance spectroscopy (EIS) was also employed to investigate the oxidation of sulfite on the FDCAMCNTPE. Figure 7 presents Nyquist diagrams and bode plots of the imaginary impedance (Z_{im}) vs. the real impedance (Z_{re}) of the EIS obtained at the modified electrode recorded at 0.4 V dc-offset in the absence (curve a) and in the presence of $1000 \mu\text{mol L}^{-1}$ sulfite (curve b) in 0.04 mol L^{-1} universal buffer (pH 7.0), respectively. In the absence of sulfite, the Nyquist diagram comprises a depressed semicircle at high frequencies, which may be related to the combination of charge transfer resistance of ferrocenedicarboxylic acid electrooxidation and the double-layer capacitance, followed by a straight line with a slope of nearly 45° . The latter is due to the occurrence of mass transport process via diffusion [45].

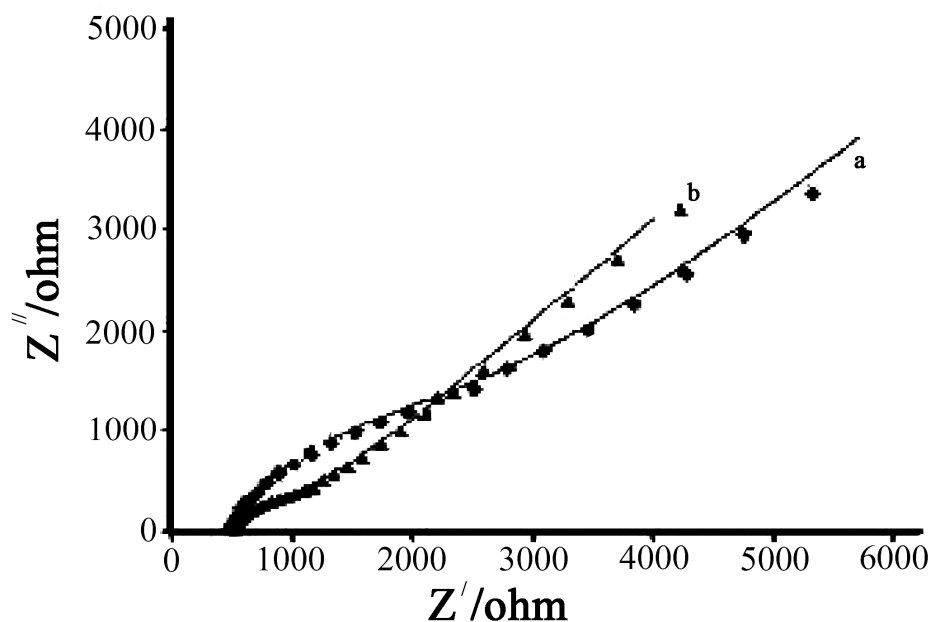
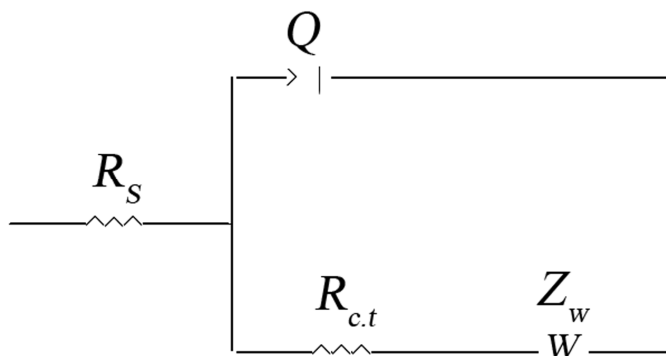


Figure 7. Nyquist diagrams of FDCAMCNTPE in the absence (a) and presence of (b) $1000.0 \mu\text{mol L}^{-1}$ sulfite. Bias is 0.4 V with $E_{ac} = 5 \text{ mV}$ with frequency range of 10 kHz to 0.1 Hz . Inset (A) shows the related bode plots of (a) and (b).



Scheme 1. Equivalent circuit for the system

The equivalent circuit compatible with the Nyquist diagram recorded in the absence and presence of sulfite is depicted in scheme 1. In this circuit, R_s , CPE, and R_{ct} represent solution resistance, a constant phase element corresponding to the double-layer capacitance, and the charge transfer resistance associated with the oxidation of low-valence ferrocenedicarboxylic acid species. W is a finite-length Warburg short-circuit term coupled to R_{ct} , which accounts for the Nernstian diffusion. In the presence of sulfite, the diameter of the semicircle decreases, confirming the electrocatalytic capability of the mentioned electrocatalyst for oxidation of sulfite. This is due to the instant chemical reaction of sulfite with the high-valence ferrocenedicarboxylic acid species. The catalytic reaction of oxidation of sulfite that occurred via the participation of ferrocenedicarboxylic acid species virtually

caused an increase in the surface concentration of low valence species of electrocatalyst, and the charge transfer resistance declined, depending on the concentration of sulfite in the solution. Impedance of CPE and W elements can be expressed as:

$$Z_{CPE} = (Y_0 j \omega)^{-n} \quad (4)$$

$$Z_W = Y_0^{-1} (j \omega)^{-1/2} \quad (5)$$

where Y_0 (the admittance parameter, $S \text{ cm}^{-2} \text{ s}^{-n}$) and n (dimensionless exponent) are two parameters independent of frequency; $j = (-1)^{1/2}$ and $\omega = \text{angular frequency} = 2\pi f$. Z_{CPE} corresponds to the constant phase angle element (CPE) impedance. $Y_0 = C_{dl}$ only when $n = 1$, and n is related to α (phase angle) by $\alpha = (1-n) 90^\circ$. So, $n = 1$ and $\alpha = 0$ stand for a perfect capacitor, and lower n values directly reflect the roughness of the electrode surface. When $n = 0.5$, it is equal to a Warburg impedance. When $n = 0$, CPE is reduced to a resistor.

4. ELECTROCATALYTIC DETERMINATION OF SULFITE

Since DPV has a much higher current sensitivity than cyclic voltammetry, we used DPV method for the determination of sulfite. The pulse height and width of 50 mV and 5 mV were selected in order to get the best sensitivity under the specific conditions. The step potential and modulation amplitude of 0.001 V and 0.05 V were selected in order to get the best sensitivity under the specific conditions. Under the optimum conditions, the response current of FDCAMCNTPE was linear with 0.6–100.0 $\mu\text{mol L}^{-1}$ sulfite concentration, with a regression equation of $I_p(\mu\text{A}) = 0.0382C_{\text{sulfite}} + 6.255$ ($r^2 = 0.9905$, $n = 11$) (Fig. 8, insert) where C_{sulfite} is concentration of sulfite in $\mu\text{mol L}^{-1}$.

The detection limits was obtained as 0.3 $\mu\text{mol L}^{-1}$ sulfite according to the definition of $Y_{LOD} = Y_B + 3\sigma$ [51].

Finally, the result of interfering studied shows that substances such as Ni^{2+} , CN^- , Ca^{2+} , Br^- , Ag^+ , $\text{S}_2\text{O}_3^{2-}$, Zn^{+2} , SO_4^{2-} , Pb^{+2} , Mn^{+2} did not any interferences (about 100-fold) for electrocatalytic determination of sulfite using FDCAMCNTPE. However, sulfide ions act as interference for determination of sulfite.

5. REAL SAMPLE ANALYSIS

In order to demonstrate the applicability of the new sensor in determining sulfite in real sample, we used the new sensor in determining of sulfite in weak liquor from the wood and paper industry and boiler water. The determination of sulfite in samples was carried out by the standard addition method for presentation of any matrix effect. Accuracy was examined by comparison of data obtained from this method with a recognized common method [52] for determination of sulfite (oxidation-reduction

titration in acid solution of KIO_3/KI in the presence of starch as indicator) (Table II). However, a group of wood extractive materials is phenolic compounds which seem electroactive. Therefore, the interference effect of some phenolic compounds such as gallic acid, ellagic acid and chrysin in the determination of sulfite in a weak liquor solution has been investigated. Our results show that those compounds do not any interference for determination of sulfite with this mediator.

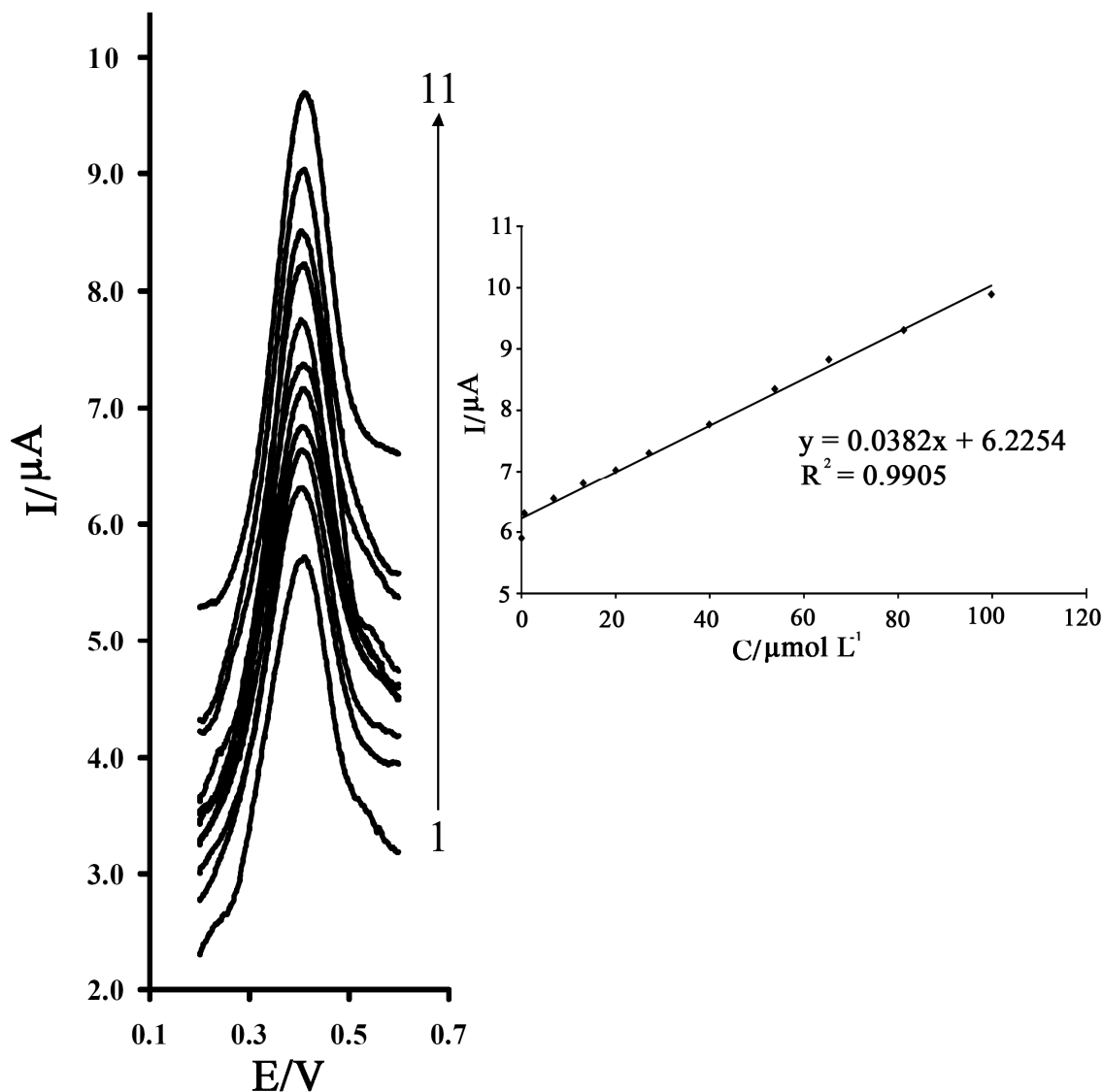


Figure 8. DPV of FDCAMCNTPE in the buffer solution ($pH\ 7.0$) containing different concentrations of sulfite. 1–11 corresponds to 0, 0.6, 7.0, 13.0, 20.0, 27.0, 40.0, 54.0, 65.0, 80.0 and $100.0\ \mu\text{mol L}^{-1}$ sulfite. Insert shows plot of electrocatalytic peak current as a function of sulfite concentration.

Table II. The results of determination of sulfite in real sample.

Sample	Sulfite found ($\mu\text{mol L}^{-1}$), proposed method	RSD%	Sulfite found ($\mu\text{mol L}^{-1}$), iodometric method	RSD%
Weak liquor 1	800	3.1	808	2.8
2	780	2.9	772	2.2
Boiler 1	3.0	3.3	3.2	2.8
2	1.9	3.2	2.2	3.1

6. CONCLUSIONS

This work demonstrates the construction of a chemically modified carbon nanotubes paste electrode by incorporation of ferrocenedicarboxylic acid as a suitable electrochemical sensor for sulfite determination at trace level. The new voltammetric method for the determination of sulfite is very rapid (less than 1 min per sample solution), reproducible, selective and sensitive and can be used for real sample analysis. The results show that the oxidation of sulfite is catalyzed at *pH* 7.0, whereas the peak potential of sulfite is shifted about 350 mV to a less positive potential at the surface of the FDCAMCNTPE. The proposed method is selective, simple and precise method for voltammetric determination of sulfite in real sample such as weak liquor from the wood and paper industry.

ACKNOWLEDGMENT

The authors wish to thank Isfahan University of Technology Research Council and the Center of Excellence in Sensor and Green Chemistry for their support.

References

1. A. Attari, B. Jaselskis, *Anal. Chem.*, 44 (1972) 1515.
2. B. S. Kumar, N. Balasubramanian, *J. AOAC. Int.*, 75 (1992) 1006.
3. C.F. Pereira, *J. Chromatogr.*, 624 (1992) 457.
4. T.J. Cardwell, M.J. Christophersen, *Anal. Chim. Acta*, 416 (2000) 105
5. S. Utzman, *J. Chromatogr.*, 640 (1993) 287.
6. S. Pozdniakova, R. Ragauskas, A. Dikcius, A. Padarauskas, *Fresenius J. Anal. Chem.*, 363 (1999) 124.
7. A. Padarauskas, V. Paliulionyte, R. Ragauskas, A. Dikcius, *J. Chromatogr. A*, 879 (2000) 235.
8. R. Makhija, A. Hitchen, *Anal. Chim. Acta*, 105 (1979) 375.
9. J. Berglund, P. Werndrup, L.I. Eiding, *J. Chem. Soc. Dalton Trans.*, 9 (1994) 1435.
10. L. Pizzoferrato, G. Di Lullo, E. Quattrucci, *Food Chem.* 63 (1998) 275.
11. M. Masař, M. Dankovař, E. Iveckař, A. Stachurovař, D. Kaniansky, B. Stanislawski, *J. Chrom. A*, 1084 (2005) 101.
12. G. Jankovskiene, Z. Daunoravicius, A. Padarauskas, *J. Chromatogr. A*, 934 (2001) 67.

13. M. Masař, M. Dankova, E. Ořivecka, A. Stachurova, D. Kaniansky, B. Stanislawski, *J. Chromatogr. A*, 1026 (2004) 31.
14. S.S.M. Hassan, M.S.A. Hamza, A.H.K. Mohamed, *Anal. Chim. Acta*, 570 (2006) 232.
15. J. Ghasemi, D.E. Mohammadi, *Anal. Lett.*, 36 (2003) 2243.
16. H. Meng, F. Wu, Z. He, Y. Zeng, *Talanta*, 48 (1999) 571.
17. R.L. Bonifácio, N. Coiche, *Anal. Chim. Acta*, 517 (2004) 125.
18. K. Matsumoto, H. Matsubara, H. Ukeda, Y. Osajima, *Agric. Biol. Chem.*, 53 (1989) 2347.
19. R. Carballo, V. Campo Dall'Orto, A. Lo Balbo, I. Rezzano, *Sens. Actuators B*, 88 (2003) 155.
20. H. Zhou, W. Yang, C. Sun, *Talanta*, 77 (2008) 366.
21. T. Garcia, E. Casero, E. Lorenzo, F. Pariente, *Sens. Actuators B*, 106 (2005) 803.
22. J. B. Raoof, R. Ojani, H. Karimi-Maleh, *Int. J. Electrochem. Sci.*, 2 (2007) 257.
23. M. Scampicchio, N.S. Lawrence, A. Arecchi, S. Mannino, *Electroanalysis*, 20 (2008) 444.
24. M.H. Pournaghi-Azar, M. Hydarpour, H. Dastango, *Anal. Chim. Acta*, 497 (2003) 33.
25. J.B. Raoof, R. Ojani, H. Karimi-Maleh, *Asian J. Chem.*, 20 (2008) 483.
26. T.R.L. Dadamos, M.F.S. Teixeira, *Electrochim. Acta*, 54 (2009) 4552.
27. M. Mazloum Ardakani, F. Habibollahi, H.R. Zare, H., *Int. J. Electrochem. Sci.*, 3 (2008) 1236.
28. E. Skavås, A. Adriaens, T. Hemmingsen, *Int. J. Electrochem. Sci.*, 1 (2006) 414.
29. E. Skavås, T. Hemmingsen, *Int. J. Electrochem. Sci.*, 2 (2007) 203.
30. J. Wang, *Electroanalysis*, 17 (2005) 7.
31. J. Wang, M. Musameh, *Anal. Chim. Acta*, 511 (2004) 33.
32. R.P. Deo, J. Wang, *Electrochem. Commun.* 6 (2004) 284.
33. J. Wang, M. Musameh, Y. Lin, *J. Am. Chem. Soc.* 125 (2003) 2408
34. H. Wang, C. Zhou, C.J. Liang, H. Yu, F. Peng, J. Yang, *Int. J. Electrochem. Sci.* 3 (2008) 1258.
35. J. Wang, M. Shi, Z. Li, N. Li, Z. Gu, *Electroanalysis*, 14 (2002) 225.
36. W. Huang, W. Hu, J. Song, *Talanta*, 61 (2003) 411.
37. P. Xiao, Q. Zhou, F. Xiao, F. Zhao, B. Zeng, *Int. J. Electrochem. Sci.*, 1 (2006) 228.
38. J. Wang, M. Li, Z. Shi, N. Li, Z. Gu, *Anal. Chem.*, 74 (2002) 1993.
39. P. Xiao, W. Wu, J. Yu, F. Zhao, *Int. J. Electrochem. Sci.*, 2 (2007) 149.
40. A. Salimi, R. Hallaj, *Talanta*, 66 (2004) 967.
41. A. Mohammadi, A.B. Moghaddam, R. Dinarvand, J. Badraghi, F. Atyabi, A. A. Saboury, *Int. J. Electrochem. Sci.*, 3 (2008) 1248.
42. H. Beitollahi, H. Karimi-Maleh, H. Khabazzadeh, *Anal. Chem.*, 80 (2008) 9848.
43. A. Salimi, M. Izadi, R. Hallaj, S. Soltanian, H. Hadadzadeh, *J. Solid State Electrochem.*, 13 (2009) 485.
44. Ali A. Ensafi, M. Taei, T. Khayamian, H. Karimi-Maleh, F. Hasanpour, *J. Solid State Electrochem.*, In press.
45. H. Karimi-Maleh, A.A. Ensafi, A.R. Allafchian, *J. Solid State Electrochem.*, 14 (2010) 9.
46. E. Mirmomtaz, A.A. Ensafi, H. Karimi-Maleh, *Electroanalysis*, 20 (2008) 1973.
47. A.A. Ensafi, H. Karimi-Maleh, *J. Electroanal. Chem.*, 640 (2010) 75.
48. M.H. Pournaghi-Azar, H. Razmi-Nerbin, *J. Electroanal. Chem.*, 488 (2000) 17.
49. H. Karimi-Maleh, A.A. Ensafi, H.R. Ensafi, *J. Braz. Chem. Soc.*, 20 (2009) 880.
50. Z. Galus, *Fundamentals of Electrochemical Analysis*, Ellis Horwood, New York. 1976.
51. J.N. Miller, J.C. Miller, *Statistics and Chemometrics for Analytical Chemistry*, 4th ed., Pearson Education Ltd., Edinburgh Gate, Harlow, Essex, England. 2000.
52. J. Berglund, P. Werndrup, L.I. Eiding, *J. Chem. Soc. Dalton Trans.*, 9 (1994) 1435.